THE JOURNAL OF PHYSICAL CHEMISTRY C

Article

Cite This: J. Phys. Chem. C 2019, 123, 13939−13943

pubs.acs.org/JPCC

Gaussian Distribution of Electron Transfer Distance in Redox Terminated Self-Assembled Thiol Monolayers

Federico G. Davia, Santiago E. Herrera,[†] and Ernesto J. Calvo*

Departamento de Química Inorgánica, Analítica y Química Física, INQUIMAE, CONICET Facultad de Ciencias Exactas y Naturales, Ciudad Universitaria, Pabellón 2, Buenos Aires C1428EHA, Argentina

Supporting Information

ABSTRACT: A Gaussian distribution of tunneling distances due to different orientation populations in electrochemically active self-assembled monolayers composed of alkanethiols of different length has been assumed in a model which leads to a Gaussian distribution of the logarithm of the electron transfer constants. The model has been validated with experimental data for osmium terminated SAMs of different length using a modification of Creager's method.

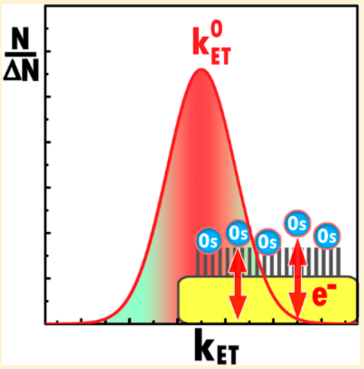

INTRODUCTION

Electrochemically active centers at terminal self-assembled monolayers (SAMs) on gold are model systems that exhibit electron transfer from the underlying metal to the terminal redox center. Control of the spacing between the redox center and the metal electrode can be achieved with high spatial resolution using variable chain length alkanethiols. For this system, the electron transfer rates decay exponentially with distance as shown in 1991 by the seminal work of Chidsey:[1]

$$k_{ET} = k^0_{ET} e^{-\beta(d-d_0)} \quad (1)$$

Here, β is the tunneling decay constant, typically 1 Å^{-1} for alkanethiol linkers;[2,3] $d - d_0$ is the tunneling distance between the electrode and the tethered redox molecule.

There is very vast literature on the electron transfer to redox centers at the end of alkanethiol self-assembled monolayers.[3−7] With the exception of the work of Creager,[8] who considered multiple independent populations of redox sites, each exhibiting the same formal potential but a unique electron transfer rate constant, the analysis of the electronic coupling versus distance has considered a single standard rate constant which implies a fixed separation between the surface and the redox molecules.

In a previous communication, we studied an outer sphere osmium bipyridine complex tethered by alkanethiols of different lengths to Au surfaces, which exhibit linear plots of ln k_{ET} vs the number of CH_2 units. However, frequency dispersion of the ET rate constants was observed which was more evident for the shortest alkanethiols.[9] With $\beta \approx 1$ Å^{-1}, very small differences in the tunneling distance due to different populations of redox molecules in slightly different configurations would result in significant variations of the ET rate constant, explaining the observed dispersion.

The dispersion of electrochemical rate constants has been studied in the past considering a Gaussian distribution of electrode potentials[10,11] or a Gaussian distribution of the logarithm of the rate constants.[12,13] In this study, we have adapted Creager's homogeneous ET transfer model (see Supporting Information) by introducing a Gaussian distribution of tunneling distances into the Randles equivalent-circuit analysis, obtaining as a result a Gaussian distribution of ET rate constant that allows a better description of the process. The model was tested experimentally by analyzing the tunneling dependence of the ET rate with the distance between a gold surface and an osmium complex covalently tethered to different length alkanethiol SAMs using electrochemical impedance spectroscopy.

EXPERIMENTAL SECTION

6-Mercaptohexanoic acid (6-MDA), 8-mercaptooctanoic acid (8-MOA), 11-mercaptoundecanoic acid (11-MUA), 16-mercaptohexadecanoic acid (16-MHDA), 1-ethyl-3-(3-dimethylamino-propyl)-carbodiimide (EDC), *N*-hydroxysuccinimide (NHS), 4-(2-hydroxyethyl) piperazine-1-ethanesulfonic acid (HEPES), potassium nitrate (KNO_3), and perchloric acid ($HClO_4$) were obtained from Sigma-Aldrich and used as received. The $Os[(bpy)_2(PyCH_2NH_2)Cl]PF_6$ complex was synthesized according to previous reports.[14,15]

Received: January 23, 2019
Revised: May 6, 2019
Published: May 6, 2019

DOI: 10.1021/acs.jpcc.9b00702
J. Phys. Chem. C 2019, 123, 13939−13943

Electroactive redox couples were attached to a spherical gold microelectrode in order to minimize non-Faradaic currents. Typically, a 400 μm diameter gold sphere (working electrode) was obtained by carefully melting the end of a 150 μm diameter gold wire using a Bunsen burner.

The gold surface modification starts with the thiol self-assembly of the acid terminated alkanethiol. For this, a freshly prepared gold sphere microelectrode was incubated for 24 h in a 5 mM ethanolic solution of each thiol and then washed with ethanol and Milli-Q water. In the next step, the carboxylic acid modified surface was activated by soaking the electrode for 30 min in a 10 mM EDC + 10 mM NHS aqueous solution. After being washed with water, the electrode was immersed in a 0.1 μM $Os[(bpy)_2(PyCH_2NH_2)Cl]PF_6$ aqueous solution containing 0.1 M KNO_3 and 10 mM HEPES buffer for 4 h to couple the $-COOH$ groups and the $-NH_2$ groups of the Os complexes.

The electrochemical experiments were performed with an Autolab V 30 (Eco Chemie, Utrecht, The Netherlands) controlled by NOVA 1.11 software. The potentiostat was equipped with a 750 kHz bandwidth ADC750 fast sampling module and a scangen analogue sweep module. All electrochemical experiments were carried out at room temperature (20 ± 2 °C) in a purpose-built three electrode glass cell. A Pt counter electrode and a Ag/AgCl, 3 M KCl reference electrode were employed, and potentials herein are reported with respect to this reference. The modified microelectrode was submerged in a 1 M $HClO_4$ aqueous solution as a low-resistance supporting electrolyte. A meniscus was formed at the contact between the electrolyte/air interface and the gold microelectrode working electrode. An ac-sinusoidal potential perturbation was then applied to the cell in a potential window between 0.05 V (fully reduced redox center) and 0.55 V (fully oxidized redox center) with a 25 mV step potential.

RESULTS AND DISCUSSION

In the present approach, instead of considering a fixed tunneling distance, we introduce a Gaussian distribution of tunneling distances, $\theta(d) = N_d/dN_d$, around an average value:

$$\theta(d) = \sum \frac{x_i}{\sigma_i\sqrt{2\pi}} e^{-[d-d_{0,i}]^2/2\sigma_i^2} \tag{2}$$

Here, $d_{0,i}$ is the average distance for the population of molecules at a tunneling distance d_i; σ_i is the standard deviation, and $x_i = \Gamma_i/\Gamma_{Tot}$ is the fraction of molecules Γ_i in that population relative to the total redox species Γ_{Tot}.

Replacing eq 2 in the tunneling expression eq 1, we obtain for the distribution of electron transfer rate constants a Gaussian distribution of the logarithm of the standard rate constants k_{ET} with a, a normalization constant. $\theta(k_{ET}) = N_k/dN_k$:

$$\theta(k_{ET}) = a\sum e^{-1/2\beta^2\sigma^2[\ln(k_{ET}/k_{ET}^0)]^2} \tag{3}$$

We have tested this hypothesis by using a modification of the method introduced by Creager and Wooster using ac-impedance spectroscopy which allows fast kinetics to be measured (i.e., $\lesssim 5 \times 10^5$ s^{-1}), with ultramicroelectrodes which decrease the double layer capacitance and the electrolyte resistance.[16] The spherical microelectrode has a very small double layer capacitance, $C_{dl} = A/(\varepsilon\varepsilon_0 d)$ with r = 200 μm and $A = 4\pi r^2$ = 0.005 cm^2, which yields a very small charging time constant.

We consider the generalized Randles equivalent-circuit depicted in Scheme 1 with different subpopulations of redox

Scheme 1. Randles Equivalent-Circuit for an Electrode Coated with a Redox-Active Monolayer Film Consisting of Different Subpopulations of Redox Molecules[6]

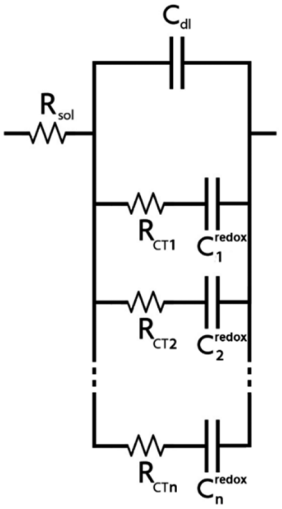

molecules.[17] By using a highly concentrated supporting electrolyte, the uncompensated solution resistance (R_{sol}) can be neglected, and the double layer capacitance C_{dl} can be obtained from the imaginary impedance at potentials far from the formal redox potential, $E \ll E^0$: $1/\mathrm{Im}(\mathbf{Z}_{E\neq E^0}) = 1/Z''_{E\neq E^0} = \omega C_{dl}$.

Without potential restrictions, the impedance of the circuit can be written as

$$\frac{1}{\mathbf{z}_{Total}} = \frac{1}{\mathbf{z}_{dl}} + \sum \frac{1}{\mathbf{z}_i} = j\omega C_{dl} + \sum \frac{1}{\mathbf{z}_i} \tag{4}$$

with

$$\mathbf{Z}_i = R_{CT,i} - \frac{1}{\omega C_{redox,i}} j \tag{5}$$

where j is the imaginary number, $j^2 = -1$:

$$C_{redox,i} = \frac{F^2 A}{RT}\frac{\Gamma_i}{\Gamma_{Total}}\Gamma_{Total} = C_{redox}x_i \tag{6}$$

and

$$R_{CTi} = \frac{1}{2C_{redox,i}k_i} = \frac{1}{2C_{redox}x_i k_i} \tag{7}$$

Assuming a continuous distribution of tunneling distances, the sums become integrals, and

$$C_{redox}(k) = C_{redox}\theta_{(k)}\,dk \tag{8}$$

$$R_{CT}(k) = \frac{1}{2C_{redox}k\theta_{(k)}\,dk} \tag{9}$$

DOI: 10.1021/acs.jpcc.9b00702
J. Phys. Chem. C 2019, 123, 13939−13943

$$\frac{1}{\mathbf{z}} = j\omega C_{dl} + C_{redox}\left[\int_0^{+\infty} \frac{\theta(k)}{2k\left(\frac{1}{4k^2} + \frac{1}{\omega^2}\right)}\,dk + \int_0^{+\infty} \frac{\theta(k)}{\omega\left(\frac{1}{4k^2} + \frac{1}{\omega^2}\right)}\,dk\right] \quad (10)$$

The improper integrals of the real and imaginary parts are $A(\omega)$ and $B(\omega)$, respectively, which can be solved numerically, and the experimental imaginary impedance ratio ξ can be fitted to the following expression:

$$\xi(\omega) = \frac{\mathbf{Z}''_{(E\neq E_0)}}{\mathbf{Z}''_{(E=E_0)}} = \frac{\left(\frac{C_{dl}}{C_{redox}}\omega + B(\omega)\right)^2 + A(\omega)^2}{\frac{C_{dl}}{C_{redox}}\omega\left(\frac{C_{dl}}{C_{redox}}\omega + B(\omega)\right)} \quad (11)$$

where

$$A = \int_0^{+\infty} \frac{\theta(k)}{2k\left(\frac{1}{4k^2} + \frac{1}{\omega^2}\right)}\,dk$$

and

$$B = \int_0^{+\infty} \frac{\theta(k)}{\omega\left(\frac{1}{4k^2} + \frac{1}{\omega^2}\right)}\,dk$$

The electron transfer for $Os[(bpy)_2(PyCH_2NH_2)Cl]PF_6$ modified self-assembled monolayers of different length alkanethiols on gold was studied by electrochemical impedance spectroscopy (EIS). A full spectrum of frequencies between 1 Hz and 100 kHz was applied at constant potential while recording phase angle ($\varnothing$), impedance module (Z), and both real (Z') and imaginary (Z'') components of the total impedance using a 10−40 mV input signal amplitude. The impedance spectrum mesurement was repeated for increasing applied potentials, scanning the entire potential window from 0.05 to 0.55 V. After the measurement, a $Z''_{E\neq E^0}/Z''_E$ vs E plot was reconstructed as depicted in Figure 1 for different frequencies.

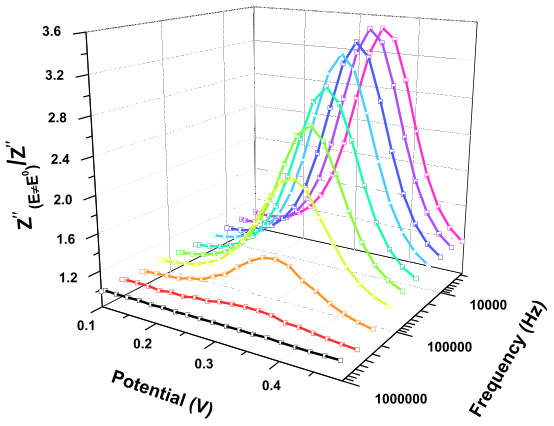

Figure 1. Plot of $Z''_{E\neq E^0}/Z''$ vs potential at different frequencies, for an Os modified 6-mercaptohexanoic acid SAM.

Plots of $Z''_{E\neq E^0}/Z''$ vs electrode potential in Figure 1 have a maximum (ξ) at the formal redox potential, E_0', determined by the electron transfer rate constant, k^0_{ET}, the double layer capacitance, C_{dl}, and the redox capacitance, C_{redox}. Figure 2

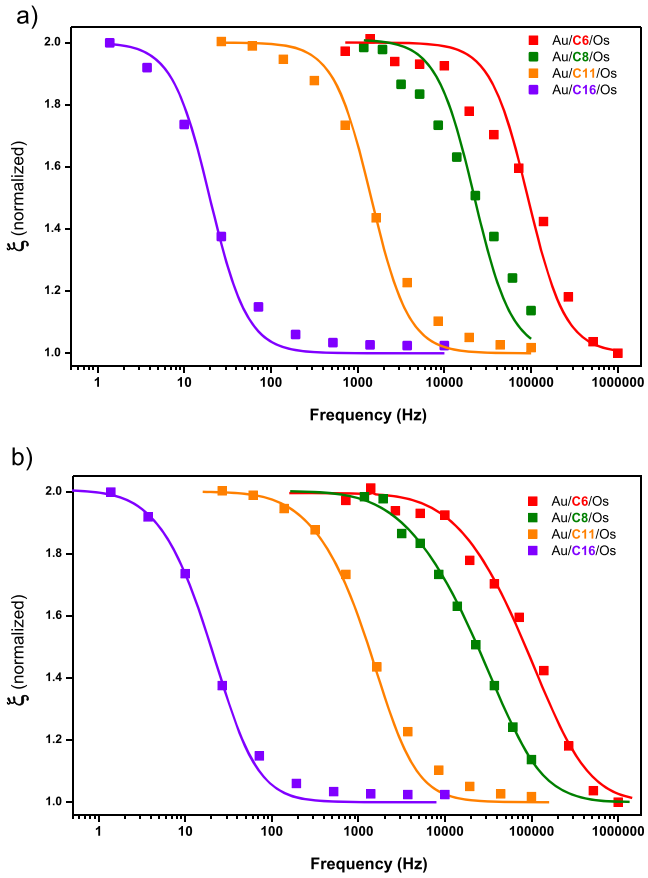

Figure 2. Frequency dependence of normalized ξ at $E^{0\prime}$ for different length Os modified SAMs on gold (C6, C8, C11, and C16) assuming a fixed distance between the redox center and the electrode[9] (a) and a Gaussian distribution of tunneling distances (b).

depicts the frequency dependence of $\xi = \frac{\mathbf{Z}''_{(E\neq E_0)}}{\mathbf{Z}''_{(E=E_0)}}$ at $E^{0\prime}$ for Os terminated C6, C8, C11, and C16 alkanethiol SAMs. While the raw data for each system is shown in Figure S1 (Supporting Information), each curve in Figure 2 has been normalized to reach $\xi = 1$ at high frequency and $\xi = 2$ at low frequency in order to compare the data for all different thiols. By fitting eq 11 to the experimental data (shown in Figure S1), we obtain C_{dl}/C_{redox}, $b = 1/2\ \beta^2\sigma^2$, and k^0_{ET}. The fitting parameters are summarized in Table 1.

In Figure 2a, assuming a fixed tunneling distance, the experimental points of ξ fall below the curve predicted by Creager's model at frequencies below the inflection point while higher experimental values of ξ were observed above the inflection point. The Gaussian distribution, on the other hand, produces a better fitting of the experimental data for all alkanethiols than the model that assumes a fixed tunneling distance. The discrepancy of the k^0_{ET} values derived by each model increases the shorter the alkanethiol is, as can be seen from Table 1.

From the fitted values of C_{dl}/C_{redox} and the double layer capacitance C_{dl}, obtained experimentally from the complex impedance at a potential far from the redox potential (−1/

DOI: 10.1021/acs.jpcc.9b00702
J. Phys. Chem. C 2019, 123, 13939−13943

Table 1. Parameters Used for the Data Fitting in Figure 2 Using Creager's Model (Fixed Distance between Electrode and Redox Molecules) and the Gaussian Distribution Model (Equation 11)

	Creager's model		Gaussian distribution		
	k^0_{ET}/s^{-1}	$\frac{C_{dl}}{C_{redox}}$	k^0_{ET}/s^{-1}	$\frac{1}{2\beta^2\sigma^2}$	$\frac{C_{dl}}{C_{redox}}$
C6	180 000	0.41	52 000	0.45	0.385
C8	38 000	0.22	125 00	0.5	0.2
C11	1700	0.14	950	0.8	0.135
C16	33	0.33	18	1	0.32

$Z''_{E\neq E^0}$ vs ω, Figure S3 in Supporting Information), the redox capacitance, C_{redox}, was evaluated as the surface redox concentration Γ_{Total} was calculated with eq 8. Table 2 shows the values of C_{dl}, C_{redox}, and osmium surface concentration, $\Gamma_{Os} \sim 4 \times 10^{-12}$ mol cm^{-2} or 0.4 μC cm^{-2}.

Table 2. Double Layer Capacity, Redox Capacity, and Surface Os Complex Concentration for Each Electrode

thiol	$C_{dl}/\mu F$	$C_{redox}/\mu F$	$\Gamma_{Os}/10^{-12}$ mol cm^{-2}
C6	0.031	0.080	4.2
C8	0.015	0.076	4.0
C11	0.015	0.113	6.0
C16	0.017	0.053	2.8

A linear plot of the natural logarithm of k^0_{ET} vs the number of CH_2 groups in the alkanethiol chain yields the value of β close to 1 (see Figure S2 in Supporting Information), and the standard deviation σ^2 was calculated using the fitting parameter $1/2\beta^2\sigma^2$.

Figure 3 depicts the distance distributions (eq 2) for each alkanethiol used and shows that the Gaussian width increases

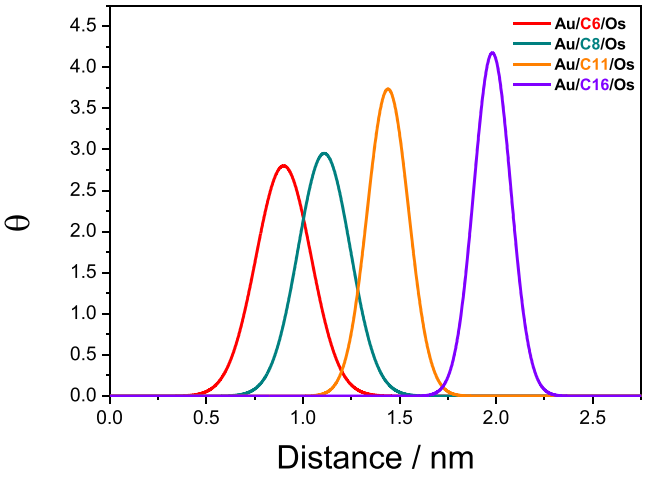

Figure 3. Distribution of distances between the redox centers and the gold surface for each electrode used.

as the length of the alkanethiol chains decreases as expected for less compact SAMs. This result is consistent with the more compact structure of longer alkanethiols due to stronger van der Waals interactions, which increase with the number of CH_2 groups.[18]

CONCLUSIONS

The frequency dispersion of tunneling standard rate constants for a series of osmium bipyridine complex tethered on Au by self-assembled alkanethiol monolayers of different lengths could be explained by a Gaussian distribution of tunneling distances. The Gaussian distribution of tunneling distances resulted in a Gaussian distribution of the logarithm of the rate constants.

An analytical solution for the impedance frequency dependence at each electrode potential has been obtained from which k^0_{ET}, C_{dl}, C_{redox}, and the standard deviation σ_k values for each thiol were obtained by nonlinear fit to the experimental data.

ASSOCIATED CONTENT

Supporting Information

The Supporting Information is available free of charge on the ACS Publications website at DOI: 10.1021/acs.jpcc.9b00702.

Homogeneous electron transfer equivalent-circuit analysis; experimental ξ data without normalization for C6, C8, C11, and C16; dependence of ln(k) vs distance; and double layer capacity calulations (PDF)

AUTHOR INFORMATION

Corresponding Author

*E-mail: calvo@qi.fcen.uba.ar.

ORCID

Ernesto J. Calvo: 0000-0003-0397-2406

Present Address

†S.E.H.: Instituto de Investigaciones Fisicoquímicas Teóricas y Aplicadas (INIFTA), Facultad de Ciencias Exactas, Universidad Nacional de La Plata—CONICET—Sucursal, 4 Casilla de Correo 16, 1900 La Plata, Argentina.

Author Contributions

All authors have given approval to the final version of the manuscript and have contributed equally.

Notes

The authors declare no competing financial interest.

ACKNOWLEDGMENTS

The authors acknowledge financial support from CONICET, ANCPCyT PICT 2016-4380, and the University of Buenos Aires. E.J.C. is a Senior Research Fellow of CONICET. S.E.H. and F.G.D. acknowledge doctoral scholarships from CONICET.

REFERENCES

(1) Chidsey, C. E. D. Free Energy and Temperature Dependence of Electron Transfer at the Metal-Electrolyte Interface. *Science* **1991**, *251*, 919−922.

(2) Miller, C. J.; Rubinstein, I. *Physical Electrochemistry*; Marcel Dekker: New York, 1995.

(3) Finklea, H. O. Electron Transfer. In *Encyclopedia of Electrochemistry*; Bard, A. J., Stratmann, M., Eds.; Wiley-VCH Verlag GmbH & Co.: Weinheim, 2007; Vol. *10*, pp 623−650.

(4) Smalley, J. F.; Finklea, H. O.; Chidsey, C. E. D.; Linford, M. R.; Creager, S. E.; Ferraris, J. P.; Chalfant, K.; Zawodzinsk, T.; Feldberg, S. W.; Newton, M. D. Heterogeneous Electron-Transfer Kinetics for Ruthenium and Ferrocene Redox Moieties through Alkanethiol Monolayers on Gold. *J. Am. Chem. Soc.* **2003**, *125*, 2004−2013.

(5) Sachs, S. B.; Dudek, S. P.; Hsung, R. P.; Sita, L. R.; Smalley, J. F.; Newton, M. D.; Feldberg, S. W.; Chidsey, C. E. D. Rates of Interfacial

DOI: 10.1021/acs.jpcc.9b00702
J. Phys. Chem. C 2019, 123, 13939−13943

Electron Transfer through Π-Conjugated Spacers. *J. Am. Chem. Soc.* **1997**, *119*, 10563−10564.
(6) Creager, S. E.; et al. Electron Transfer at Electrodes through Conjugated "Molecular Wire" Bridges. *J. Am. Chem. Soc.* **1999**, *121*, 1059−1064.
(7) Smalley, J. F.; Feldberg, S. W.; Chidsey, C. E. D.; Linford, M. R.; Newton, M. D.; Liu, Y. P. The Kinetics of Electron Transfer through Ferrocene-Terminated Alkanethiol Monolayers on Gold. *J. Phys. Chem.* **1995**, *99*, 13141−13149.
(8) Li, J.; Schuler, K.; Creager, S. E. Generalized Equivalent-Circuit Model for Electroactive Monolayers Exhibiting a Fixed Redox Potential and a Distribution of Electron-Transfer Rate Constants. I. Square Distributions. *J. Electrochem. Soc.* **2000**, *147*, 4584−4588.
(9) Herrera, S.; Adam, C.; Ricci, A.; Calvo, E. J. Electrochemical Gating of Single Osmium Molecules Tethered to Au Surfaces. *J. Solid State Electrochem.* **2016**, *20*, 957−967.
(10) Sabatani, E.; Anson, F. C. Mediated Electron Transfer across Nafion Solution Interfaces. Comparison with Marcus Theory for Cases Involving Gaussian Arrays of Mediator Couples. *J. Electroanal. Chem.* **1995**, *386*, 111−119.
(11) Albery, W. J.; Boutelle, M. G.; Colby, P. J.; Hillman, A. R. The Kinetics of Electron Transfer in the Thionine-Coated Electrode. *J. Electroanal. Chem. Interfacial Electrochem.* **1982**, *133*, 135−145.
(12) Nahir, T. M.; Bowden, E. F. The Distribution of Standard Rate Constants for Electron Transfer between Thiol-Modified Gold Electrodes and Adsorbed Cytochrome C. *J. Electroanal. Chem.* **1996**, *410*, 9−13.
(13) Albery, W. J.; Bartlett, P. N.; Wilde, C. p.; Darwent, J. R. A General Model for Dispersed Kinetics in Heterogeneous Systems. *J. Am. Chem. Soc.* **1985**, *107*, 1854−1858.
(14) Danilowicz, C.; Corton, E.; Battaglini, F. Osmium Complexes Bearing Functional Groups: Building Blocks for Integrated Chemical Systems. *J. Electroanal. Chem.* **1998**, *445*, 89.
(15) Ricci, A. M.; Bonazzola, C.; Calvo, E. J. *Phys. Chem. Chem. Phys.* **2006**, *8*, 4297.
(16) Creager, S. E.; Wooster, T. T. A New Way of Using Ac Voltammetry to Study Redox Kinetics in Electroactive Monolayers. *Anal. Chem.* **1998**, *70*, 4257−4263.
(17) Creager, S. E.; Wooster, T. T. A New Way of Using Ac Voltammetry to Study Redox Kinetics in Electroactive Monolayers. *Anal. Chem.* **1998**, *70*, 4257−4263.
(18) Grumelli, D.; Méndez De Leo, L. P.; Bonazzola, C.; Zamlynny, V.; Calvo, E. J.; Salvarezza, R. C. Methylene Blue Incorporation into Alkanethiol Sams on Au(111): Effect of Hydrocarbon Chain Ordering. *Langmuir* **2010**, *26*, 8226−8232.

DOI: 10.1021/acs.jpcc.9b00702
J. Phys. Chem. C 2019, 123, 13939−13943